NASA

National Aeronautics and
Space Administration

NASA CR-165438

ANALYSIS OF INTERFACE CRACKS IN ADHESIVELY BONDED LAP SHEAR JOINTS

Final Report - Part IV

by

S.S. Wang and J.F. Yau

Department of Theoretical and Applied Mechanics
UNIVERSITY OF ILLINOIS
at Urbana-Champaign

prepared for

NATIONAL AERONAUTICS AND SPACE ADMINISTRATION

NASA Lewis Research Center
Grant NSG 3044

1. Report No.	2. Government Accession No.	3. Recipient's Catalog No.
NASA CR 165438		

4. Title and Subtitle	5. Report Date
Analysis of Interface Cracks in Adhesively Bonded Lap Shear Joints	February 1981
	6. Performing Organization Code
7. Author(s)	8. Performing Organization Report No.
S. S. Wang and J. F. Yau	
	10. Work Unit No.
9. Performing Organization Name and Address	
University of Illinois Urbana, IL 61801	11. Contract or Grant No. NSG 3044
	13. Type of Report and Period Covered
12. Sponsoring Agency Name and Address	Final Report - Part IV
National Aeronautics and Space Administration Washington DC 20546	14. Sponsoring Agency Code

15. Supplementary Notes
Project Manager: C. C. Chamis, Structures & Mechanical Technologies Division
NASA Lewis Research Center, Mail Stop 49-6
21000 Brookpark Road
Cleveland, OH 44135

16. Abstract

The conservation laws of elasticity for nonhomogeneous materials developed under this grant are used to study the crack behavior in adhesively bonded lap shear joints. These laws and the fundamental relationships in fracture mechanics of interface cracks, the problem is reduced to a pair of linear algebraic equations, and stress intensity solutions can be determined directly by information extracted from the far field. The numerical results obtained show that: (1) in the lap-shear joint with a given adherend, the opeining-mode stress intensity factor, (K_I) is always larger than that of the shearing-mode (K_{II}); (2) K_I is not sensitive to adherent thickness but K_{II} increases rapidly with increasing thickness; and (3) K_I and K_{II} increase simultaneously as the interfacial crack length increases.

17. Key Words (Suggested by Author(s))	18. Distribution Statement
stress intensities, surface energies, theory of elasticity, nonhomogeneous materials, fracture mechanics opening mode, shearing mode, finite element	Unclassified, Unlimited

19. Security Classif. (of this report)	20. Security Classif. (of this page)	21. No. of Pages	22. Price*
Unclassified	Unclassified		

* For sale by the National Technical Information Service, Springfield, Virginia 22161

TABLE OF CONTENTS

FOREWORD

This report describes a portion of the results obtained on NASA Grant NSG 3044. This work was done under subcontract to the University of Illinois, Urbana, with Prof. S.S. Wang as the Principal Investigator. The prime grantee was the Massachusetts Institute of Technology, with Prof. F.J. McGarry as the Principal Investigator and Dr. J.F. Mandell as a major participant. The NASA - LeRC Project Manager was Dr. C.C. Chamis.

Efforts in this project are primarily directed towards the development of finite element analyses for the study of flaw growth and fracture of fiber composites. This report presents a method of analysis for adhesive or interlaminar cracks which propagate in the interface, rather than cohesively in the adhesive or interlayer. The latter case was treated in an interim report NASA CR-135248.

ABSTRACT

A study on the elastic behavior of interface cracks in adhesively bonded lap shear joints is presented. The problem is investigated by using a recently developed method of analysis based on conservation laws in elasticity for nonhomogeneous solids and fundamental relationships in fracture mechanics of dissimilar materials. The formulation leads to a pair of linear algebraic equations in mixed-mode stress intensity factors. Singular crack-tip stress intensity solutions are determined directly by information extracted from the far field. Stress intensity factors and associated energy release rates are obtained for various cases of interest. Fundamental nature of the interfacial flaw behavior in lap-shear adhesive joints is examined in detail.

1. INTRODUCTION

While adhesively bonded joints have been employed in many secondary structural components, the effective use of adhesive joining technology in primary load-bearing structural members is still in its infancy. Applications of adhesive joints will not reach their full potential until certain critical problems are solved. The major factors responsible for this situation are the complex failure modes and mechanics presented in the joints. Because of many geometric, material and fabrication variables involved, the fracture problem of adhesive joints is extremely complicated. Current knowledge of the joint failure behavior is yet very limited. Analyses and design criteria for flaw resistance of adhesively bonded joints are seriously deficient.

Interfacial cracking, also called debonding, is one of the most frequently encountered modes of failure. It frequently occurs at geometric boundaries such as edges and re-entry corners due to inherent stress concentrations, or results from faulty joining in fabrication such as incomplete wetting between adherend and adhesive. Debonding is also found in adhesive joints subjected to combined high temperature and moisture absorption. Progressive reduction of stiffness, exposure of the interior of the composite to environmental attack, and final disintegration of the structure are frequently observed to occur by the presence and growth of interfacial cracks. The lap-shear joint shown in Fig. 1 is considered in this study, because it is one of the most widely used joint configuration in structural applications. Understanding the fundamental nature of interfacial cracks is of utmost importance in the reliability and safety design of the adhesive joints for primary load-bearing structures. In this paper

analytical study on the interfacial crack behavior in the adhesively bonded lap-shear joints is presented.

The interface crack problem was apparently first studied by Williams [1]. Elasticity theories for cracks of this nature were attempted by many investigators, and solutions characteristically involve oscillatory stress singularity [2-7]. A major concern for the oscillation of near-field stresses is that they lead to physical absurdity of crack surface interpenetration or overlapping, as pointed out by England [2] and Malyshev, et al. [8]. This implies that the solutions for the interface crack problem are physically inadmissible. The unsatisfactory aspects of the oscillatory stress singularity were discussed by several researchers, for example, Refs. [2,8-10]. An alternate model of a closed crack tip with frictionless contact was first proposed by Comninou [9] to correct these effects. The stress singularity of the model is different from that of the oscillatory one with a finite normal tensile traction ahead of the crack tip. The crack tip in a nominal tensile field has an extremely small contact area in comparison to the size of the crack. Recently, Achenbach, et al. [10] and Keer, et al. [11] proposed another models which include the crack face closure, relative slip conditions at the interface, and different definitions of stress intensity factors. In view of the complexities aforementioned, the interfacial crack problem in adhesively bonded joints is obviously rather difficult. The complex structural geometry, the presence of the multiphase material system, and the unknown multiaxial stress state acting on the crack introduce additional complications. The very local nature of the interface crack singularity as shown in [7,12] is noted to introduce the thickness of the thin adhesive layer as a characteristic dimension in the problem. Any simplifications, which fail to consider the

crucial role of the thin adhesive layer, would lead to a severe drawback in studying the full nature of the adhesive joint fracture. The importance and complexities of interface debonding in adhesive joints have long been recognized [13-15]. However, research progress on this kind of real-life defect has been relatively slow.

In this paper, a study on the interfacial crack behavior in adhesively bonded lap-shear joints is presented. By using the recently developed conservation laws of elasticity for nonhomogeneous solids [16-20] and fundamental relationships in fracture mechanics of interface cracks, the problem is reduced to a pair of linear algebraic equations, and stress intensity solutions can be determined directly by information extracted from the far field. This feature makes the current approach particularly suitable and attractive. Solutions are obtained for adhesively bonded lap-shear joints with various material systems and geometric configurations of the crack and the joint. The method of analysis is of practical use in the design and analysis of adhesive joint fracture. The fundamental nature and unique features of the interface flaw behavior in adhesively bonded joints are revealed.

2. FORMULATION

The Eshelby-Rice conservation law for a homogeneous solid in a plane elasticity problem [16-19] has recently been extended to a solid composed of two dissimilar materials [20] with the following form:

$$J_i\{S\} = \int_S (W\, n_i - \sigma_{jk}\, n_k\, u_{j,i})ds - \int_\ell ([W]\delta_{i2} - \sigma_{j2}[u_{j,i}])ds = 0, \qquad (1)$$

where W is the strain energy density; σ_{jk}, the stress tensor; u_j, the displacement vector; n_i, the outward unit normal of an arbitrary closed contour S which encloses a portion of the continuum, and ℓ is a portion of the interface bounded by S as shown in Fig. 2. The bracket [ ] in Eq. 1 denotes the jump of a function across the interface $x_2 = 0$, i.e.,

$$[W] = W(x_1,0^+) - W(x_1,0^-), \qquad (2)$$

$$[u_{j,i}] = u_{j,i}(x_1,0^+) - u_{j,i}(x_1,0^-). \qquad (3)$$

Continuity conditions of displacements and interlaminar stresses across $x_2 = 0$ require

$$[u_j] = 0 \qquad \text{and} \qquad [\sigma_{j2}] = 0. \qquad (4a,b)$$

The J_1 component of the conservation integral in Eq. 1 can be simplified to

$$J_1\{S\} = \int_S (W\, n_1 - \sigma_{jk}\, n_k\, u_{j,1})ds = 0, \qquad (5)$$

which is the same as the analogous result for a single phase material.

For a solid containing an interface crack between two dissimilar materials as shown in Fig. 3, J_1 in Eq. 5 along a path Γ has the standard J-integral form in homogeneous fracture mechanics, i.e.,

$$J \equiv J_1\{\Gamma\} = \int_\Gamma (W dx_2 - T_i \frac{\partial u_i}{\partial x_1} ds), \tag{6}$$

where Γ is an arbitrary path surrounding the crack tip, provided that the crack surfaces are free from traction and the interface is a straight line. [Path independent integrals (similar to Rice's J-integral of course with appropriate modifications) for elastic media with spatially varying moduli were noted by Atkinson [21] through an energy-momentum tensor formalism.] The J is shown to relate to the energy release rate G of an interface crack in a usual manner, i.e.,

$$J = G = G_I + G_{II}, \tag{7}$$

where G_I and G_{II} are the energy release rates associated with the mode I and mode II stress intensity factors. The interface crack-tip stress intensity factors, K_I and K_{II}, are defined in a complex form as

$$K_I - i\, K_{II} = 2\sqrt{2\pi}\, e^{\beta\pi} \lim_{z\to o} z^{\frac{1}{2}+i\beta}\, \Phi_1(z), \tag{8}$$

where $\Phi_1(z)$ is a complex potential in the well-known Kolosov-Muskhelishvili formulation [3,22], and β is a bimaterial constant given in Ref. [3].

It is noted that K_I and K_{II} defined in Eq. 8 for an interfacial crack in dissimilar media are different from those for a crack in a homogeneous solid. Thus, the K_I and K_{II} may not possess the usual significance and physical interpretation as in the cohesive (or homogeneous) fracture. While the overall stress intensity factor [3,23] may be used to express the maximum amplitude of stresses and to correlate crack extension, accurate description of the oscillatory singular stress field in the neighborhood of the crack tip requires detailed knowledge of individual stress intensity factors. Because of the complexity of the problem, numerical procedures are necessary

for obtaining accurate solutions for interface crack problems. For example, Lin and Mar [24] used a hybrid-stress finite element method to achieve this. Hong and Stern [23] employed a contour integral method based on Betti's Reciprocal work theorem and, recently, Smelser [25] used crack-flank displacement data provided by numerical solutions to yield the interface crack-tip stress intensities. Each of these numerical approaches requires its own computational scheme to handle the problem and has given satisfactory results. In this section, an alternate and convenient method of analysis is proposed for determining the interfacial K_I and K_{II} in bonded joints.

Using the stress field established by Rice et al. [3], one can readily show that the J-integral in Eq. 7 is related to the stress intensity factors for an interfacial crack by

$$J = \sum_{i=1}^{2} \frac{1 - \nu_i}{4\mu_i}(K_I^2 + K_{II}^2) \tag{9}$$

for a plane strain case. The coefficients in Eq. 9 are replaced by $1/[4\mu_i (1 + \nu_i)]$ for a plane stress condition. The J-integral *alone* does not provide adequate information for determining individual values of K_I and K_{II} for an inherently, mixed-mode interfacial crack. Further development of Eq. 9 based on the introduction of known auxiliary solutions for the crack problem can remove this difficulty.

Consider two independent equilibrium states with associated field variables denoted by superscripts 1 and 2 for the elastically deformed bimaterial body. Superposition of the two equilibrium states leads to another equilibrium state, 0. The J-integral for the superimposed state can be shown to have the form

$$J^{(0)} = J^{(1)} + J^{(2)} + M^{(1,2)}, \tag{10}$$

where $M^{(1,2)\dagger}$ is another conservation integral with the form

$$M^{(1,2)} = \int_{\Gamma} \left(W^{(1,2)} \, dx_2 - \left[T_i^{(1)} \frac{\partial u_i^{(2)}}{\partial x_1} + T_i^{(2)} \frac{\partial u_i^{(1)}}{\partial x_1} \right] ds \right) . \tag{11}$$

The $W^{(1,2)}$ in Eq. 11 is the mutual potential energy density of the bimaterial body, defined by

$$W^{(1,2)} = C_{ijk\ell} \, u_{i,j}^{(1)} \, u_{k,\ell}^{(2)} = C_{ijk\ell} \, u_{i,j}^{(2)} \, u_{k,\ell}^{(1)} . \tag{12}$$

Recalling the J-K relationship in Eq. 9 for the superimposed state and comparing it with Eq. 10, one can obtain

$$M^{(1,2)} = 2\alpha \left[K_I^{(1)} \, K_I^{(2)} + K_{II}^{(1)} \, K_{II}^{(2)} \right] \tag{13}$$

where

$$\alpha = \sum_{i=1}^{2} \frac{1}{4\mu_i} (1 - \nu_i) . \tag{14}$$

The M-integrals in Eqs. 11 and 13 deals with interaction terms only, and are used directly in solving the interface crack problem. The M-integral is clearly related to the details of the stresses and deformation at the crack tip (i.e., K_I and K_{II} in Eq. 13), but yet may be evaluated in the far field (i.e., the integral in Eq. 11), where such a calculation can be carried out with greater accuracy and convenience than near the crack tip. It is also noted that, while K_I and K_{II} characterize the controversial near-field oscillatory singular stresses, the energy release rate G, and, perhaps, G_I and G_{II}, are quantities well defined and can be evaluated conveniently mathematically and physically.

---

†The M-integral used here and elsewhere in this paper is defined by Eq. 11, and should not be confused with those in Refs. [17] and [18].

3. SOLUTION PROCEDURE

Equation 11 together with Eq. 13 provides sufficient information for determining the stress intensity solutions for a mixed-mode interface crack problem, when known auxiliary solutions are introduced. Denote the first auxiliary solution by a superscript 2a for a crack between two dissimilar materials subjected to mode-I loading only with

$$K_I^{(2a)} = 1 \qquad \text{and} \qquad K_{II}^{(2a)} = 0 \,. \tag{15}$$

Equation 13 can be simplified to

$$M^{(1,2a)} = 2\alpha \, K_I^{(1)}, \tag{16}$$

where $M^{(1,2a)}$ has the same form as Eq. 11 with the subscript 2 being replaced by 2a. $T_i^{(1)}$ and $u_i^{(1)}$ in Eq. 11 can be determined along a properly selected integration path Γ in the far field by any convenient method such as the commonly used finite element analysis. For a plane crack problem with the loading of Eq. 15, $T_i^{(2a)}$ and $u_i^{(2a)}$ are derivable by the Kolosov-Muskhelishvili formulation, and the auxiliary solution has the following form:

$$u_i^{(2a)} = \sqrt{\frac{r}{2\pi}} \, f_i^{(I)}(\ell n \, r, \, \theta; \, \mu_1, \, \nu_1, \, \mu_2, \, \nu_2), \tag{17}$$

$$T_i^{(2a)} = \sigma_{ij}^{(2a)} \, n_j, \tag{18}$$

with

$$\sigma_{ij}^{(2a)} = \frac{1}{\sqrt{2\pi r}} \, g_{ij}^{(I)}(\ell n \, r, \, \theta, \, \mu_1, \, \nu_1, \, \mu_2, \, \nu_2) + O(1) \,. \tag{19}$$

Exact forms of the functions $f_i^{(I)}$ and $g_{ij}^{(I)}$ may be found in [3,4].

The second auxiliary solution, denoted by the superscript 2b, for the bimaterial solid under a pure-mode II loading such that

$$K_I^{(2b)} = 0 \qquad \text{and} \qquad K_{II}^{(2b)} = 1, \tag{20}$$

can be found by the same formulation. The conservation integral is, therefore, expressed by

$$M^{(1,2b)} = 2\alpha\, K_{II}^{(1)}, \tag{21}$$

where $M^{(1,2b)}$ has a form similar to that of Eq. 11.

It is important to note that the auxiliary solutions, $u_i^{(2a)}$, $T_i^{(2a)}$ and $u_i^{(2b)}$, $T_i^{(2b)}$, are independent of the particular boundary-value problem being posed. Therefore, they may be determined independently by any convenient analytical method once for all. In solving for $K_I^{(1)}$ and $K_{II}^{(1)}$, the integrals, $M^{(1,2a)}$ and $M^{(1,2b)}$, must be evaluated accurately and explicitly. For a given crack geometry, loading condition and bimaterial constant, this can be achieved by integrating Eqs. 16 and 21 along a properly selected contour in the far field so as to avoid crack-tip complications. In conjunction with the auxiliary solutions determined, a numerical method, using a conventional finite-element approach, is currently employed to calculate $T_i^{(1)}$ and $u_i^{(1)}$. The M-integrals are then formally evaluated by using the second-order Gaussian quadrature along a contour Γ passing through Gaussian stations of each element (Fig. 4).

4. NUMERICAL RESULTS AND DISCUSSION

The solution procedure aforementioned is programmed for studying general two-dimensional interface crack problems. Evaluation of the conservation integrals is conducted in conjunction with a conventional finite element method by using eight-node isoparametric elements. Solutions are obtained for lap-shear joints with various adherends, adhesives, and geometric configurations. Accuracy and convergence of the results are affected by several unusual features of the problem and the method of analysis due to the singular nature of the crack and inherent approximation involved in the numerical evaluation of the conservation integrals. Assessments of solution accuracy are made by examining relevant problems for which unquestionably correct and exact solutions are available in the literature. Excellent agreement is obtained between current results and reference solutions. Details of the study are reported elsewhere [26]. Current results have an accuracy within approximately three percent deviation from reference solutions based on the optimum mesh and the integration contour presently selected. The primary objectives of this section are to determine stress intensity solutions, which characterize local stresses and deformation, and to examine effects of material and geometric variables on the crack-tip response. Of particular interest are the complex failure modes and energy release rates associated with the interface crack.

4.1 Interfacial crack and Joint Configuration

The lap-shear joint considered in Fig. 1 is composed of two high-stiffness and high-strength adherends bonded by a thin adhesive layer. The upper and lower adherends and the adhesive layer are assumed to have uniform

thicknesses of t_1, t_3 and t_2, respectively. The overlap region has a dimension L. A crack of length a is located along the interface of the upper adherend and the adhesive near the traction-free edge. Except for the interfacial crack, perfect bonding is assumed everywhere. The two adherends are made of materials with elastic constants E_1, ν_1 and E_3, ν_3, and the thin adhesive layer has properties of E_2 and ν_2. The adhesive and adherends are assumed to be linear, elastic. Studies of related cases such as the center-of-bond cohesive crack and the eccentric crack problems were reported elsewhere [27-28].

4.2 Effects of Adhesive Properties on Interfacial Crack-Tip Response

Geometric variables in the problem are given as the following:

$$\theta = 45°, \quad L = 0.5 \text{ in.},$$
$$t_1 = t_3 = 0.05 \text{ in.}, \; t_2 = 0.005 \text{ in.}, \tag{22}$$
$$a = 2.5\, t_2 = 0.0125 \text{ in.}$$

The upper and lower adherends are made of the same aluminum with elastic constants, $E_1 = E_3 = 10 \times 10^6$ psi, and $\nu_1 = \nu_3 = 0.33$. Effects of different kinds of adhesive on the crack-tip response are examined by considering various values of E_2. For the purpose of generality, adhesives with a broad range of modulus values covering three decades on a logarithmic scale are studied. The cases with $E_1/E_2 = 20 \sim 40$ are typical for aluminum/epoxy systems. Higher E_1/E_2 values correspond to the joints with less rigid adhesives or subjected to a "hot and wet" environment.

Crack-tip stress intensity solutions and associated energy release rates are obtained as functions of the modulus ratio shown in Figs. 5 and 6. Failure modes in the joints are observed clearly. The interfacial crack

experiences a mixed-mode fracture even under uniaxial loading. Both K_I and K_{II} decrease rapidly as the adhesive modulus decreases, and the difference between K_I and K_{II} increases with E_1/E_2. The mode-I stress intensity factor is higher than that of the mode-II in the entire range studied, except for the cases of $E_1/E_2 \simeq 1$. This suggests that the dominant mode of failure is opening-mode. In the case of $E_1/E_2 = 1$, the crack is cohesive, and the nature of the crack-tip singularity changes. The values of K_I and K_{II} in this case are found to be consistent with the results in [27]. The total energy release rate and the energy release rate of individual fracture mode are determined also. For given adherends, the reduction of E_2 increases the coefficients of K_I and K_{II} in Eq. 9, which influence the G value significantly. The G_I is found to increase rapidly with E_1/E_2; G_{II}, on the other hand, decreases as a less stiff adhesive is used. The rapid increase of G_I and G corresponds to a decrease of K_I and K_{II} in the interface crack problem—a unique phenomenon not observed in the homogeneous crack problem in general. In the case of very large E_1/E_2, the adhesive may become incompressible with Poisson's ratio approaching 0.5. The incompressibility of the soft adhesive is not considered in the present study.

4.3 Effects of Dissimilar Adherends

Effects of dissimilar adherends on the interface crack behavior are studied for lap-shear joints with the same geometry and crack length used in the previous section. The adhesive layer and the lower adherend have the following elastic properties: $E_2 = 0.5 \times 10^6$ psi, $\nu_2 = 0.35$ and $E_3 = 10 \times 10^6$ psi, $\nu_3 = 0.33$. The problem is solved by considering the joints with various E_1's ranging from $E_1/E_2 = 1$ to 1000. The results

are given in Figs. 7 and 8, in which K_I, K_{II}, G_I, G_{II} and G are related to E_1/E_2 in semi-logarithmic plots. Adherends with dissimilar properties are found to have significant effects on the crack-tip response. The opening-mode stress intensity factor increases appreciably but the shearing-mode stress intensity remains relatively constant as the stiffness of the upper adherend approaches that of the lower one, i.e., $E_1/E_2 \to 20$. As E_1/E_2 exceeds 20, an opposite trend of changes of K_I and K_{II} are observed; K_I remains relatively unchanged and K_{II} increases gradually. The ratio of K_I/K_{II} in the joint with dissimilar adherends is always smaller than, or at most equal to, that of a joint with the same upper and lower adherends. Effects of dissimilar adherends on energy release rates are shown in Fig. 8. The G_I is approximately one order of magnitude larger than G_{II} in the entire range of $E_1/E_2 > 20$. The total energy release rate increases rapidly initially, and then remains relatively constant with the change of E_1/E_2. As the stiffness of the upper adherend exceeds that of the lower one, crack resistance of the joint becomes less sensitive to the dissimilarity of the two adherends. But a higher fracture resistance is obtainable as the upper adherend becomes less stiff.

4.4 Effects of Adhesive-Layer Thickness

Effects of the adhesive-layer thickness on fracture of the joint have long been recognized. Bascom, et al., for example, [13,14] showed experimentally that fracture energy release rates are related closely to the bond thickness. Extensive analytical studies on debonded composite laminates were conducted by Erdogan [5,6,29]. Several unique features of the geometric variable on the composite failure behavior were revealed. Wang, et al. [27] studied center-of-bond cohesive cracks and reported fundamental

characteristics of thickness effects on the adhesive joint fracture. In this portion of the study, lap-shear joints with a geometric configuration and crack length identical to the one used in previous sections are considered. The joints are made of identical aluminum adherends and epoxy adhesive with elastic constants: $E_1 = E_3 = 10 \times 10^6$ psi, $\nu_1 = \nu_3 = 0.33$, and $E_2 = 0.5 \times 10^6$ psi, $\nu_2 = 0.35$, respectively. The adhesive thicknesses, ranging from $t_1/40$ to $t_1/5$ (i.e., from 0.00125 in. to 0.01 in.), are considered.

Relationships among K_I, K_{II}, G_I, G_{II}, G and the normalized bond thickness, t_2/t_1 (with $t_1 = t_3 = 0.05$ in.) are shown in Figs. 9 and 10. The K_I is found to be insensitive to the change of the adhesive-layer thickness, but K_{II} increases rapidly with t_2. Quantitatively, K_I is always larger than K_{II} in all cases studied. This is particularly true for the joint with a thinner adhesive, in which K_I has a value about one order of magnitude higher than that of K_{II} in general. The K_I clearly dominates the fracture of the joint with a thinner bond, but the shearing mode failure becomes increasingly important as the adhesive thickness increases. Associated energy release rates are given in Fig. 10 for joints with various t_2/t_1's. The decrease of the adhesive-layer thickness leads to an increase of fracture resistance in the joints (i.e., a reduction in the total energy release rate and the maximum cleavage stress). The change of fracture resistance with the bond-line thickness in a lap-shear joint is consistent with the results reported in Ref. [29]. However, variations of interfacial crack-tip stress intensity factors and associated energy release rates are different from the solutions obtained for center-of-bond cohesive crack problems, in which K's and G's are almost independent of the adhesive-layer thickness. This situation is expected as stress singularities are different in the two cases.

4.5 Effects of Crack Length

Effects of the interface crack length are of significant interest because of the particular joint configuration and the loading condition applied. The geometry of the lap-shear joint studied in this section is identical to that in the previous cases. The two adherends are the same aluminum, and the adhesive is an epoxy resin with material constants reported previously. Solutions obtained for various crack lengths are reported in Figs. 11 and 12, in which K and G are related to a/L. Both K_I and K_{II} shown in Fig. 11 increase rapidly for shorter cracks (e.g., $a/L < 0.02$), and change almost linearly as a/L becomes longer. The opening-mode stress intensity factor is approximately four times higher than that of the shearing-mode in the entire range of a/L studied. Effects of the crack length on energy release rates are shown in Fig. 12. Well defined relationships are observable. In the case of a very short crack, i.e., $a \to 0$, there exists a strong interaction between the crack tip and the edges of the joint. Basic nature of the short interfacial crack and its interaction with geometric boundaries are currently under investigation.

5. SUMMARY AND CONCLUSIONS

An investigation of the interfacial crack behavior in adhesively bonded lap-shear joints is presented. The method of analysis is formulated on the basis of conservation laws in elasticity of nonhomogeneous solids and fundamental relationships in fracture mechanics of interface cracks. The current approach provides a convenient and accurate means to examine the basic nature of interface cracks in adhesive joints. Fracture parameters such as stress intensity factors and associated energy release rates describing crack-tip deformation and stresses are determined. Complex failure modes in the joints are studied. Solutions are obtained for problems with various kinds of adhesive and adherends, joint configurations and interfacial crack lengths. Based on the results obtained, the following conclusions may be drawn:

1. Adhesive properties have significant effects on the interfacial crack tip response. In the lap-shear joint with a given adherend, the opening-mode stress intensity factor is always larger than that of the shearing-mode. The difference between K_I and K_{II} increases with E_1/E_2. While both K_I and K_{II} decrease with decreasing E_2, the total energy release rate and that associated with the opening-mode fracture increase rapidly - a phenomenon unique to the interface crack and not observed in homogeneous crack problems in general.

2. The change of two identical adherends to dissimilar ones influences appreciably the failure behavior of the joints. K_I increases rapidly but K_{II} remains relatively constant as the stiffness of the upper adherend approaches that of the lower one. An opposite trend in the changes of K_I and K_{II} is observed as $E_1/E_2 > 20$. As E_1/E_2 exceeds 20, crack

resistance of the joints becomes relatively insensitive to the dissimilarity of the two adherends. The joint has a higher fracture resistance as the upper adherend becomes less stiff than the lower one.

3. Effects of the adhesive layer thickness on interfacial fracture are different from those on a center-of-the-bond cohesive crack in lap-shear joints. K_I is shown to be insensitive to the change of the adhesive thickness, but K_{II} increases appreciably. The decrease of the adhesive thickness leads to an increase of fracture resistance in the joint due to reduction of crack extension driving force.

4. Increasing the interfacial crack length increases K_I and K_{II} simultaneously. However, stress intensity solutions increase more rapidly for shorter cracks than for longer ones. For the cases of $a/L > 0.02$, approximately linear relationships between K's and a/L are observed. In a semi-logarithmic plot, G_I, G_{II} and G vary with a/L almost linearly too, suggesting that well defined relations among them may exist.

6. ACKNOWLEDGMENTS

The authors wish to express their deep gratitude to Professor H. T. Corten, Department of Theoretical and Applied Mechanics, University of Illinois, for his fruitful discussion and encouragement during the course of this study. The computational work was carried out in the Digital Computer Laboratory of the University of Illinois and supported in part by the Research Board of the University and by NASA-Lewis Research Center through Grants NSG 3044.

7. REFERENCES

[1] M. L. Williams, "The Stress Around a Fault or Crack in Dissimilar Media," *Bulletin of the Seismological Society of America*, 49 (1959 199-204.

[2] A. H. England, "A Crack Between Dissimilar Media," *Journal of Applied Mechanics*, 32, Trans. ASME Ser. E (1965) 400-411.

[3] J. Rice and G. C. Sih, "Plane Problems of Cracks in Dissimilar Media," *Journal of Applied Mechanics*, 32, Trans. ASME, Ser. E (1965) 418-423.

[4] E. Erdogan, "Stress Distribution in Bonded Dissimilar Material with Cracks," *Journal of Applied Mechanics*, 32, Trans. ASME, Ser. E (1965) 403-410.

[5] E. Erdogan and G. D. Gupta, "Stress Analysis of Multilayered Composites with a Flaw," *International Journal of Solids and Structures*, 7 (1971) 39-61.

[6] E. Erdogan and G. D. Gupta, "Layered Composites with an Interfacial Flaw," *International Journal of Solids and Structures*, 7 (1971) 1089-1107.

[7] M. Rusen Gecit and E. Erdogan, "The Effect of Adhesive Layer on Crack Propagation in Laminates," NASA Technical Report, Grant NGR 39-007-011, Department of Mechanical Engineering and Mechanics, Lehigh University, March (1976).

[8] B. M. Malyshev and R. L. Salganik, "The Strength of Adhesive Joints Using the Theory of Fracture," *International Journal of Fracture Mechanics*, 1, 2, June (1965) 114-128.

[9] M. Comninou, "The Interface Crack," *Journal of Applied Mechanics*, 44, 4, December (1977) 631-636.

[10] J. D. Achenbach, et al., "Loss of Adhesion at the Tip of an Interface Crack," *Journal of Elasticity*, 9 (1979) 397-424.

[11] A. F. Mak and L. M. Keer, "A No-Slip Edge Crack on a Bimaterial Interface," *Journal of Applied Mechanics*, , Trans. ASME, Ser. E (1981).

[12] S. S. Wang, J. F. Mandell and F. J. McGarry, "An Analysis of the Crack-Tip Stress Field in DCD Adhesive Fracture Specimens," *International Journal of Fracture*, 14, 1, February (1978) 39-58.

[13] W. D. Bascom, C. O. Timmons and R. L. Jones, "Apparent Interfacial Failure in Mixed-Mode Adhesive Fracture," *Journal of Materials Science*, 10 (1975) 1037-1048.

[14] W. D. Bascom, R. L. Cottington, R. L. Jones and P. Peyser, "The Fracture of Epoxy and Elastomer Modified Epoxy Polymers in Bulk and as Adhesives," *Journal of Polymer Science*, 19 (1975) 2545-2562.

[15] M. L. Williams, "Application of Continuum Mechanics in Adhesive Fracture," *Journal of Adhesion*, 4 (1972) 381-421.

[16] J. D. Eshelby, "The Continuum Theory of Lattice Defects," *Solid State Physics*, Eds., F. Seitz and D. Turnbull, 3, Academic Press, N. Y. (1956) 79-144.

[17] J. K. Knowles and E. Sternberg, "On a Class of Conservation Laws in Linearized and Finite Elastostatics," *Archive for Rational Mechanics and Analysis*, 44 (1972) 187-211.

[18] B. Budiansky and J. Rice, "Conservation Laws and Energy Release Rates," *Journal of Applied Mechanics*, 40, Trans ASME, Ser. E (1973) 201-203.

[19] F. H. K. Chen and R. T. Shield, "Conservation Law in Elasticity of the J-Integral Type," *Journal of Applied Mathematics and Physics (ZAMP)*, 28 (1977) 1-22.

[20] R. E. Smelser and M. E. Gurtin, "On the J-Integral for Bimaterial Bodies," *International Journal of Fracture*, 13 (1977) 382-286.

[21] C. Atkinson, "Some Results on Crack Propagation in Media with Spatially Varying Elastic Moduli," *International Journal of Fracture*, 11, 4, August (1975) 619-628.

[22] N. I. Muskhelishvili, *Some Basic Problems of Mathematical Theory of Elasticity*, P. Noordhoff, Groningen, The Netherlands (1963).

[23] C. C. Hong and M. Stern, "The Computation of Stress Intensity Factors in Dissimilar Materials," *Journal of Elasticity*, 8, 1 (1978) 21-34.

[24] K. Y. Lin and J. W. Mar, "Finite Element Analysis of Stress Intensity Factors for Cracks at Bimaterial Interface," *International Journal of Fracture*, 12, 4, August (1976) 521-531.

[25] R. E. Smelser, "Evaluation of Stress Intensity Factors for Bimaterial Bodies Using Numerical Crack Flank Displacement Data," *International Journal of Fracture*, 15, 2, April (1979) 135-143.

[26] S. S. Wang and J. F. Yau, "An Analysis of Interfacial Cracks Based on Conservation Laws in Elasticity," to appear in *International Journal of Solids and Structures* (1981).

[27] S. S. Wang, J. F. Mandell, T. H. Christesen and F. J. McGarry, "Analysis of Lap Shear Adhesive Joints With and Without Short Edge Cracks," Research Report R76-2, Department of Materials Science and Engineering, Massachusetts Institute of Technology, Cambridge, MA (1976).

[28] S. S. Wang, J. F. Mandell and F. J. McGarry, "Effects of Crack Elevation in TDCB Adhesive Fracture Tests," Research Report R76-3, Department of Materials Science and Engineering, Massachusetts Institute of Technology, Cambridge, MA (1976).

[29] F. Erdogan, "Fracture Problems in Composite Materials," *Engineering Fracture Mechanics*, 4, 4 (1972) 811-840.

8. LIST OF FIGURE CAPTIONS

Fig. 1 Coordinates and Crack Geometry in Lap Shear Adhesive Joint

Fig. 2 Integration Path S for J_i in Bi-Material Composite

Fig. 3 Interface Crack between Bonded Dissimilar Adherend and Adhesive Layer, and Path Γ for J and M Integrals

Fig. 4 Gaussian Stations, Finite Element Mesh and Path for M Integral around Interface Crack Tip

Fig. 5 Stress Intensity Factors for Interface Crack in Lap Shear Joints with Various Adhesive Moduli ($E_1 = E_3 = 10 \times 10^6$ psi, $\nu_1 = \nu_3 = 0.33$)

Fig. 6 Energy Release Rates for Interface Crack in Lap Shear Joints with Various Adhesive Moduli ($E_1 = E_3 = 10 \times 10^6$ psi, $\nu_1 = \nu_3 = 0.33$)

Fig. 7 Effects of Adherend Properties on Stress Intensity Factors for Interface Crack in Lap Shear Joints ($E_2 = 0.5 \times 10^6$ psi, $\nu_2 = 0.35$, $E_3 = 10 \times 10^6$ psi, $\nu_3 = 0.33$)

Fig. 8 Effects of Adherend Properties on Energy Release Rates for Interface Crack in Lap Shear Joints ($E_2 = 0.5 \times 10^6$ psi, $\nu_2 = 0.35$, $E_3 = 10 \times 10^6$ psi, $\nu_3 = 0.33$)

Fig. 9 Effects of Adhesive Layer Thickness t_2 on Crack-Tip Stress Intensity Factors in Lap Shear Joints ($t_1 = t_3 = 0.05$ in, $E_1 = E_3 = 10 \times 10^6$ psi, $\nu_1 = \nu_3 = 0.33$, $E_2 = 0.5 \times 10^6$ psi, $\nu_2 = 0.35$)

Fig. 10 Effects of Adhesive Layer Thickness t_2 on Energy Release Rates in Lap Shear Joints ($t_1 = t_3 = 0.05$ in, $E_1 = E_3 = 10 \times 10^6$ psi, $\nu_1 = \nu_3 = 0.33$, $E_2 = 0.5 \times 10^6$ psi, $\nu_2 = 0.35$)

Fig. 11 Stress Intensity Factor Solutions vs. Interface Crack Length in Lap Shear Adhesive Joints ($L = 0.5$ in, $E_1 = E_3 = 10 \times 10^6$ psi, $\nu_1 = \nu_3 = 0.33$, $E_2 = 0.5 \times 10^6$ psi, $\nu_2 = 0.35$)

Fig. 12 Energy Release Rates vs. Interface Crack Length in Lap Shear Adhesive Joints ($L = 0.5$ in, $E_1 = E_3 = 10 \times 10^6$ psi, $\nu_1 = \nu_3 = 0.33$, $E_2 = 0.5 \times 10^6$ psi, $\nu_2 = 0.35$)

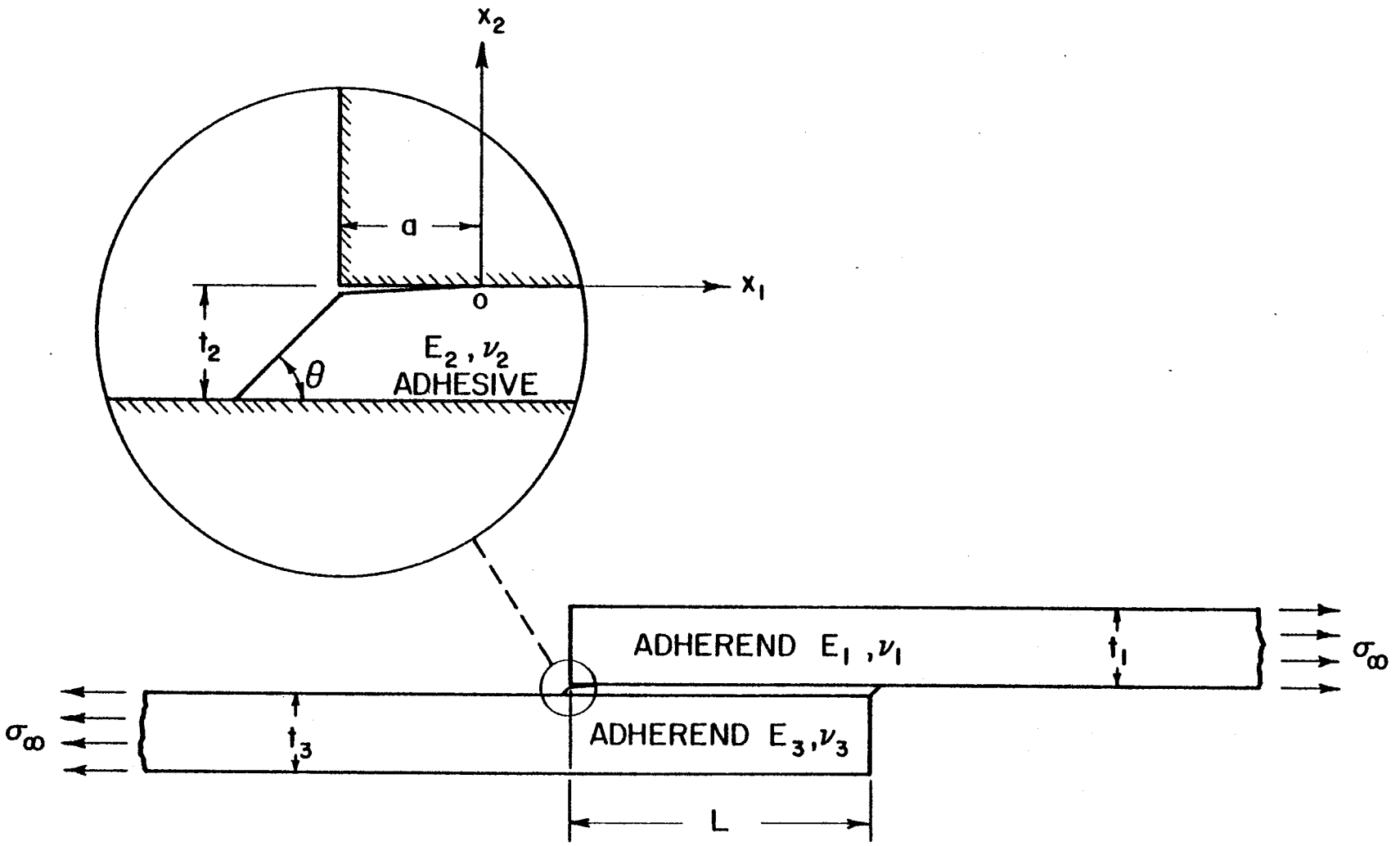

Fig. 1 Coordinates and Crack Geometry in Lap Shear Adhesive Joint

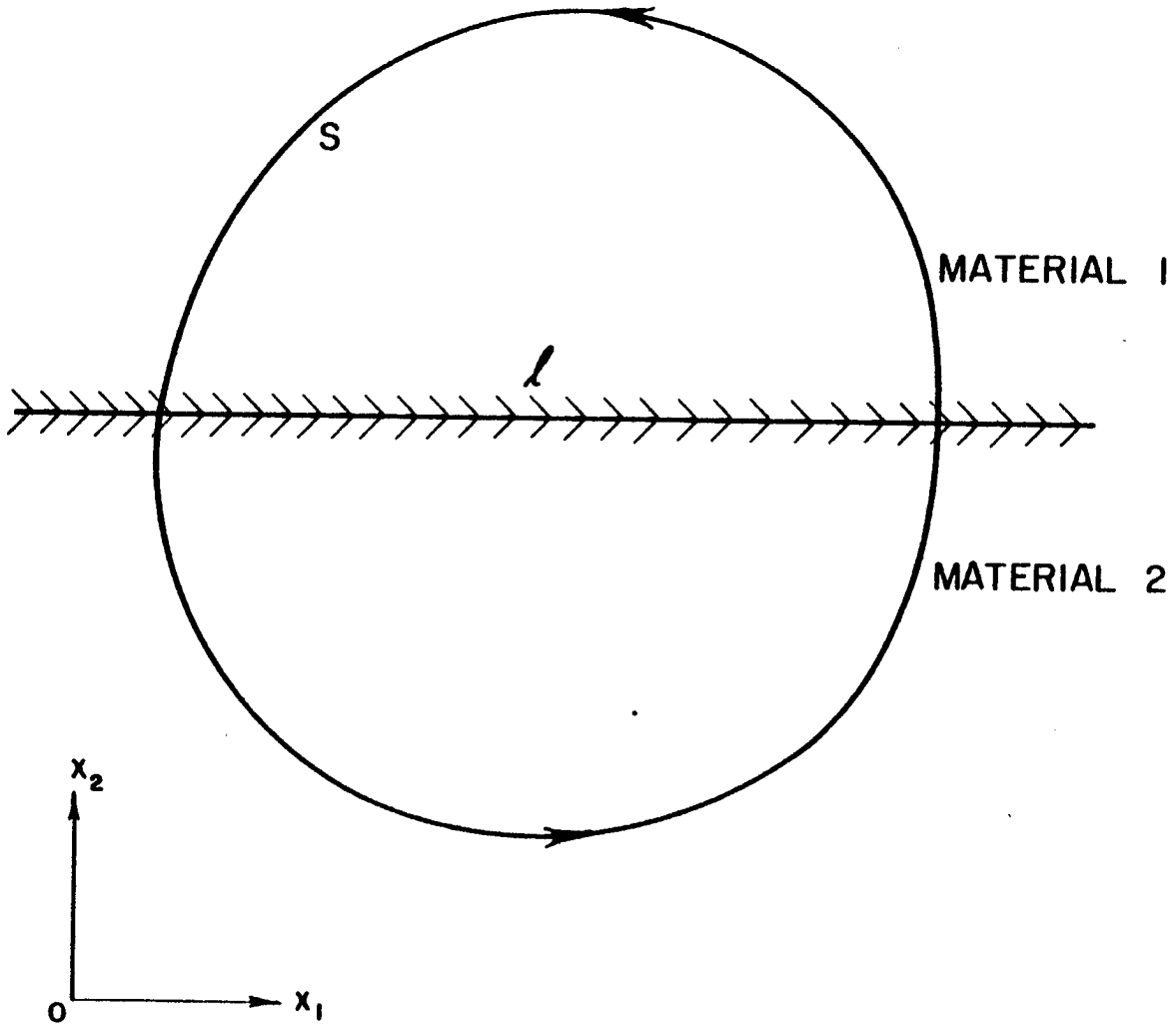

Fig. 2 Integration Path S for J_i in Bi-Material Composite

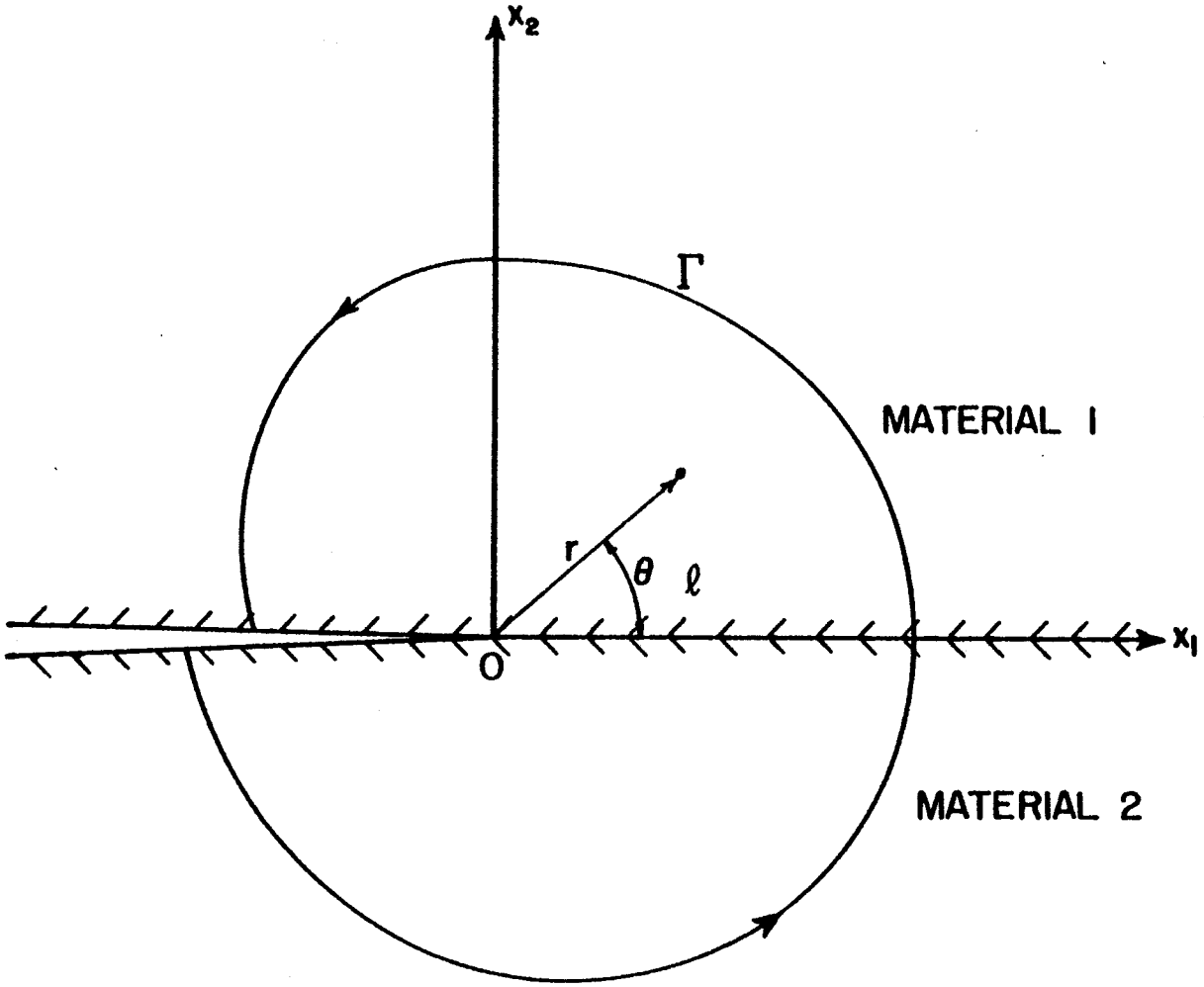

Fig. 3 Interface Crack Between Bonded Dissimilar Adherend and Adhesive Layer and Path Γ for J and M Integrals

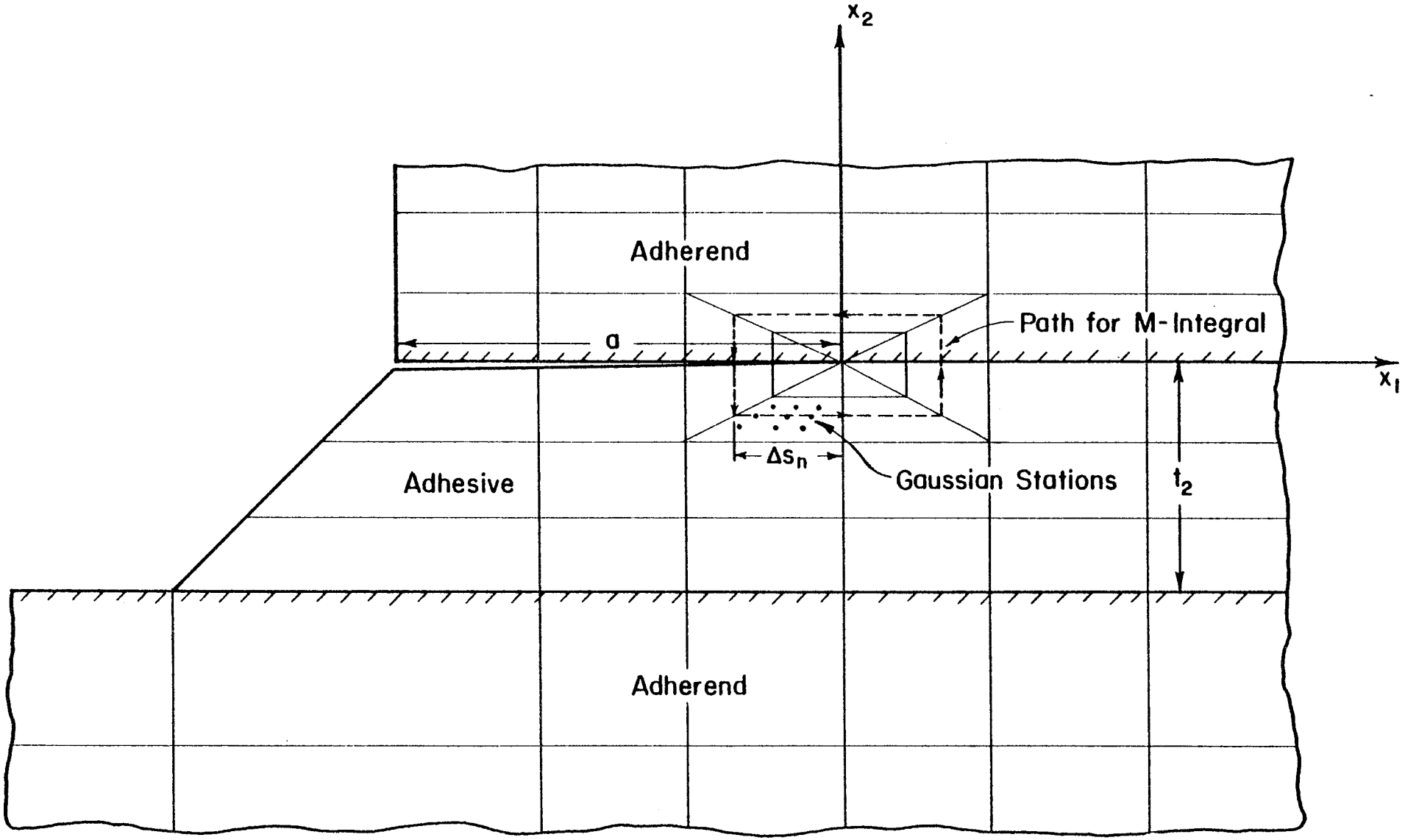

Fig. 4 Gaussian Stations, Finite Element Mesh and Path for M Integral Around Interface Crack Tip

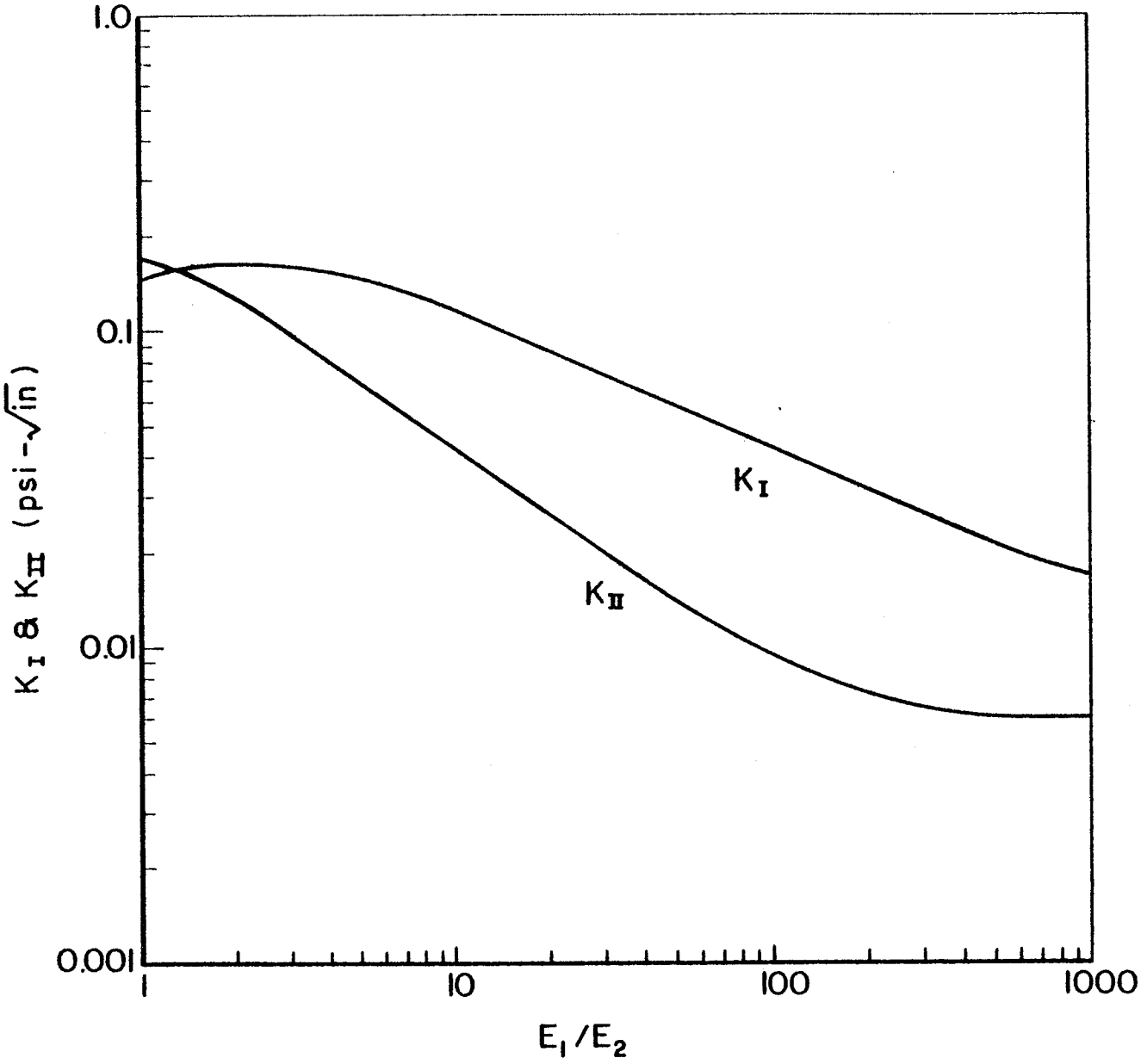

Fig. 5 Stress Intensity Factors for Interface Crack in Lap Shear Joints with Various Adhesive Moduli ($E_1 = E_3 = 10\times10^6$ psi, $\nu_1 = \nu_3 = 0.33$)

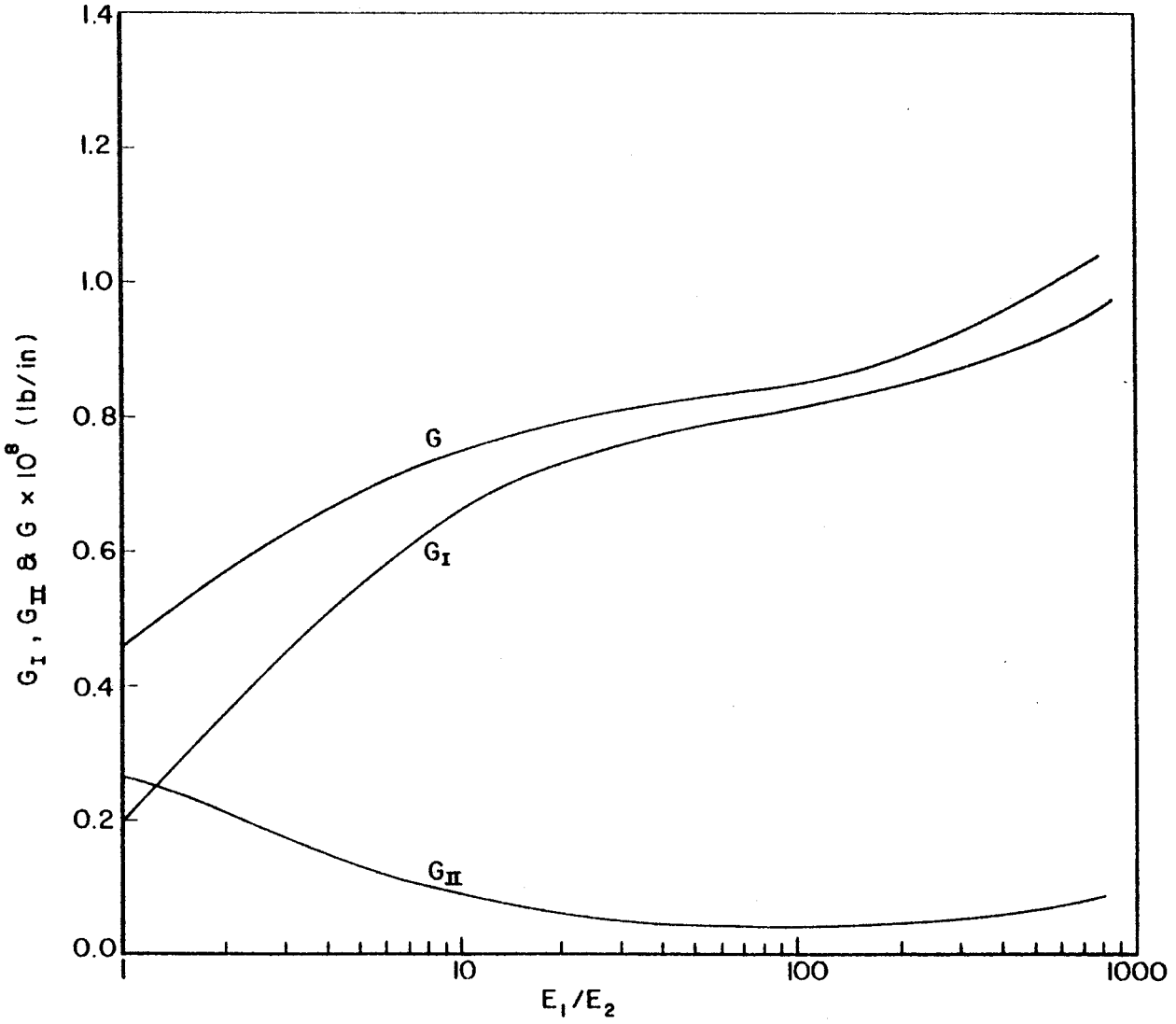

Fig. 6 Energy Release Rates for Interface Crack in Lap Shear Joints with Various Adhesive Moduli ($E_1 = E_3 = 10\times10^6$ psi, $\nu_1 = \nu_3 = 0.33$)

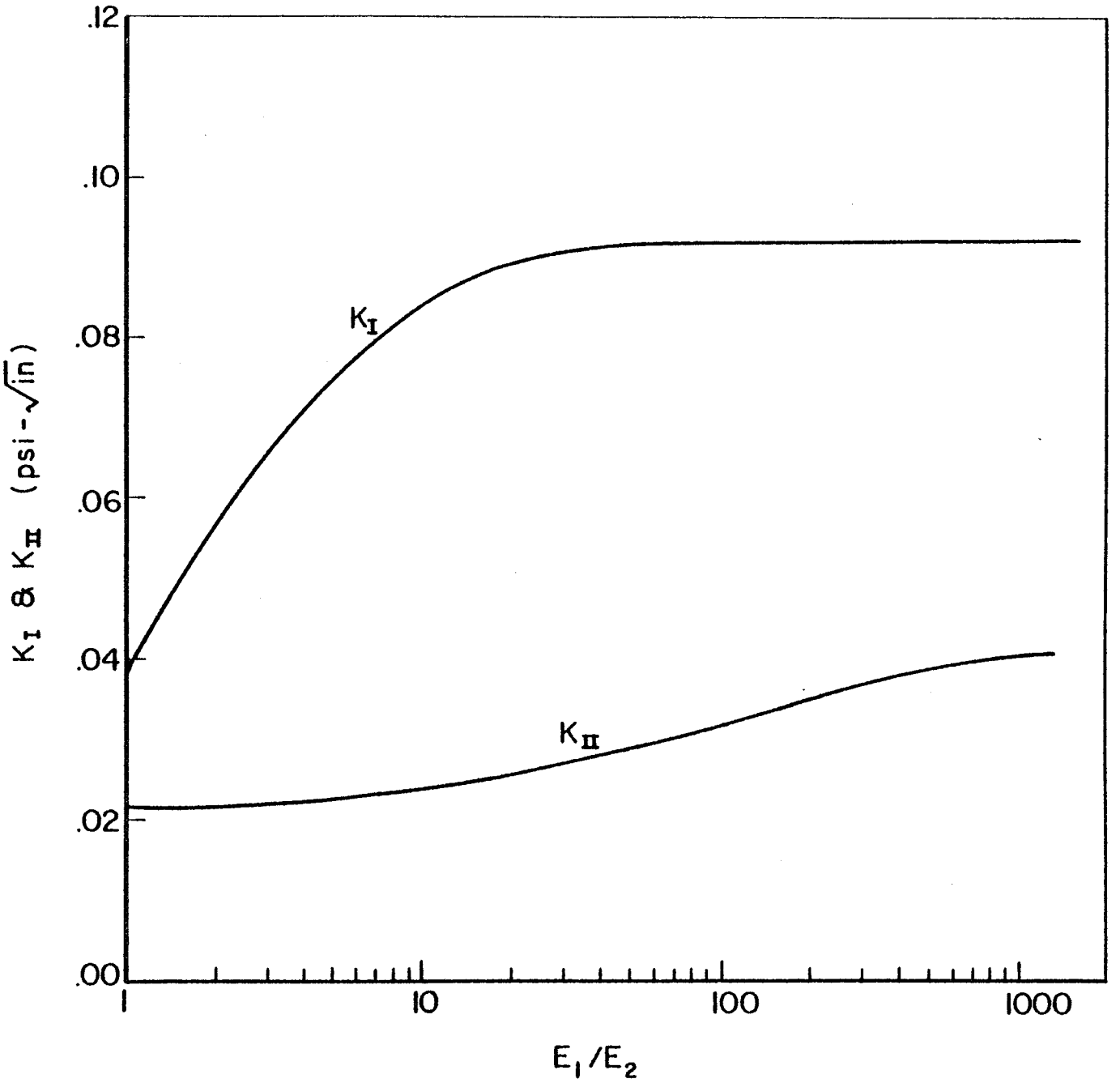

Fig. 7 Effects of Adherend Properties on Stress Intensity Factors for Interface Crack in Lap Shear Joints (E_2= 0.5×10^6 psi, ν_2= 0.35, E_3= 10×10^6 psi, ν_3= 0.33)

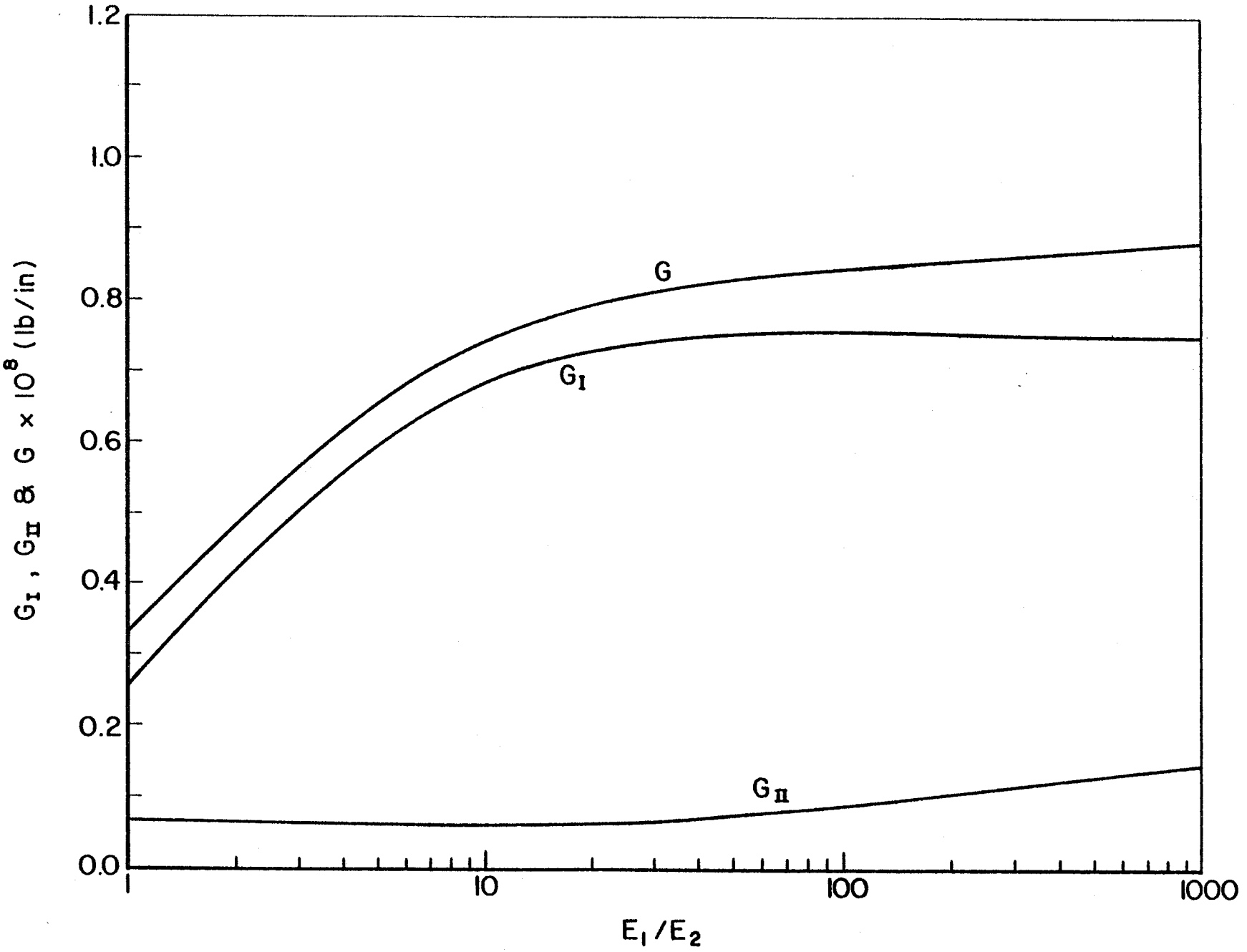

Fig. 8 Effects of Adherend Properties on Energy Release Rates for Interface Crack in Lap Shear Joints (E_2= 0.5×10^6 psi, ν_2=0.35, E_3= 10×10^6 psi, ν_3= 0.33)

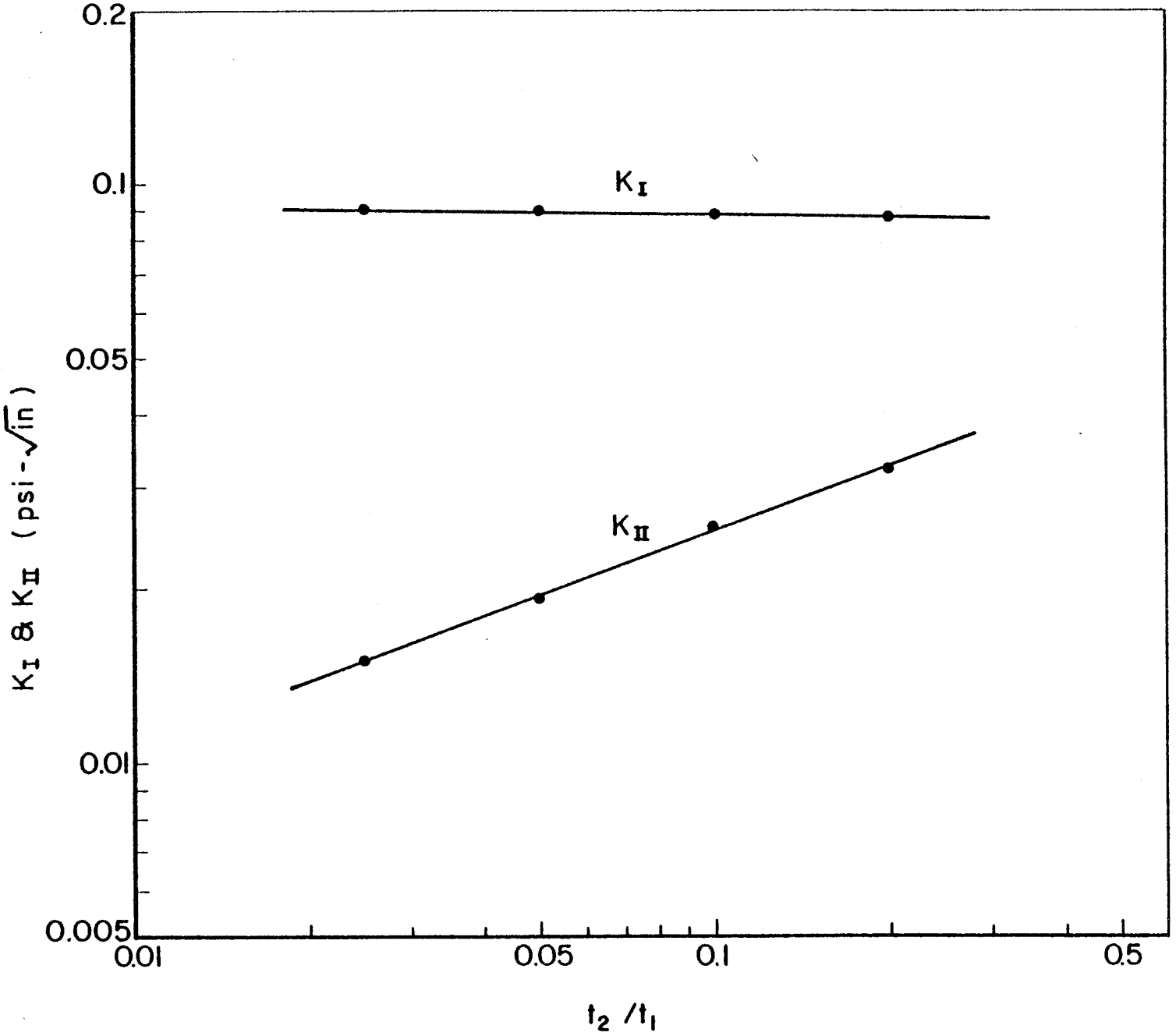

Fig. 9 Effects of Adhesive Layer Thickness t_2 on Crack-Tip Stress Intensity Factors in Lap Shear Joints (t_1= t_3= 0.05 in, E_1= E_3= 10×10^6 psi, ν_1= ν_3= 0.33, E_2= 0.5×10^6 psi, ν_2= 0.35)

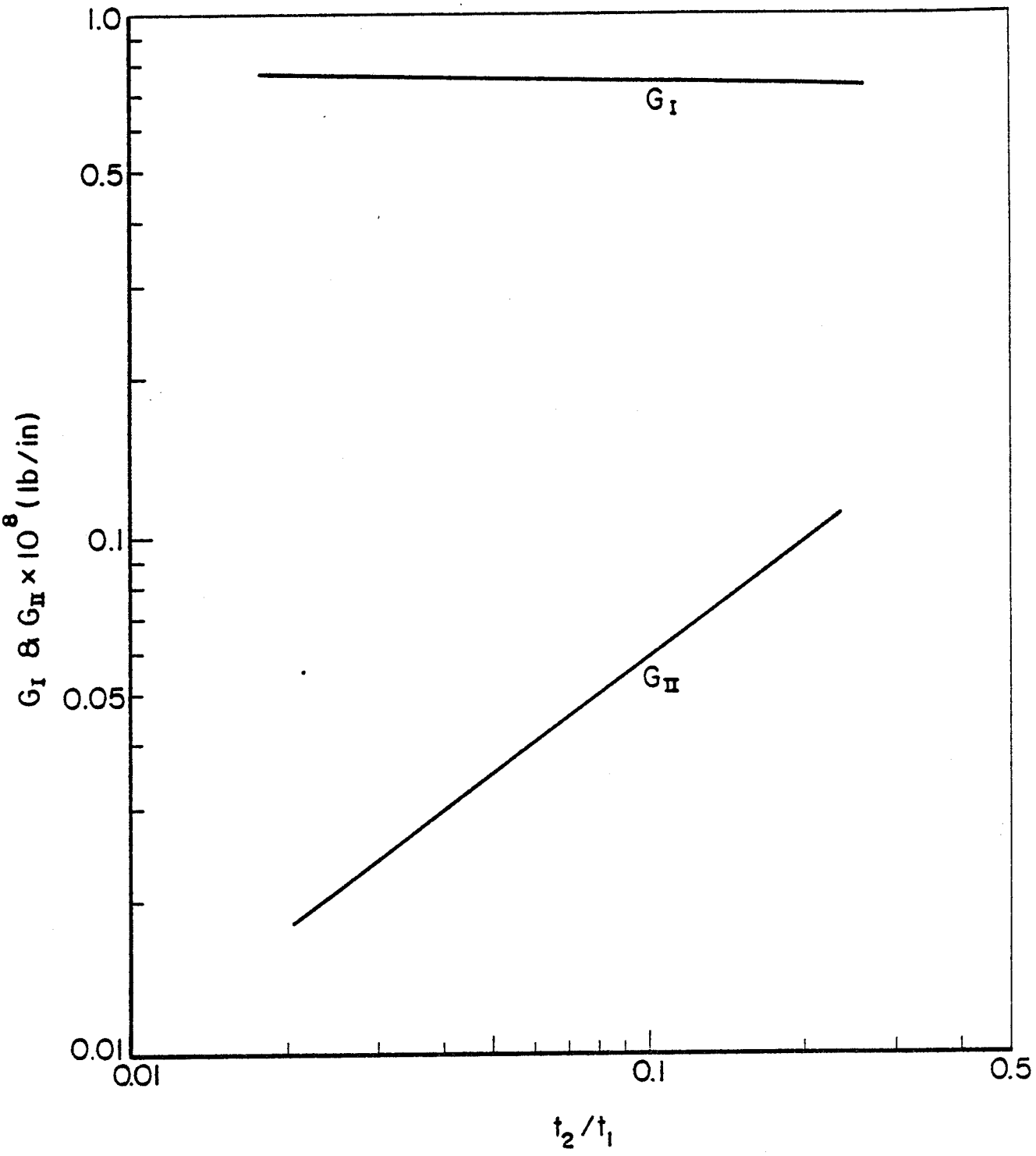

Fig. 10 Effects of Adhesive Layer Thickness t_2 on Energy Release Rates in Lap Shear Joints ($t_1 = t_3 = 0.05$ in, $E_1 = E_3 = 10 \times 10^6$ psi, $\nu_1 = \nu_3 = 0.33$, $E_2 = 0.5 \times 10^6$ psi, $\nu_2 = 0.35$)

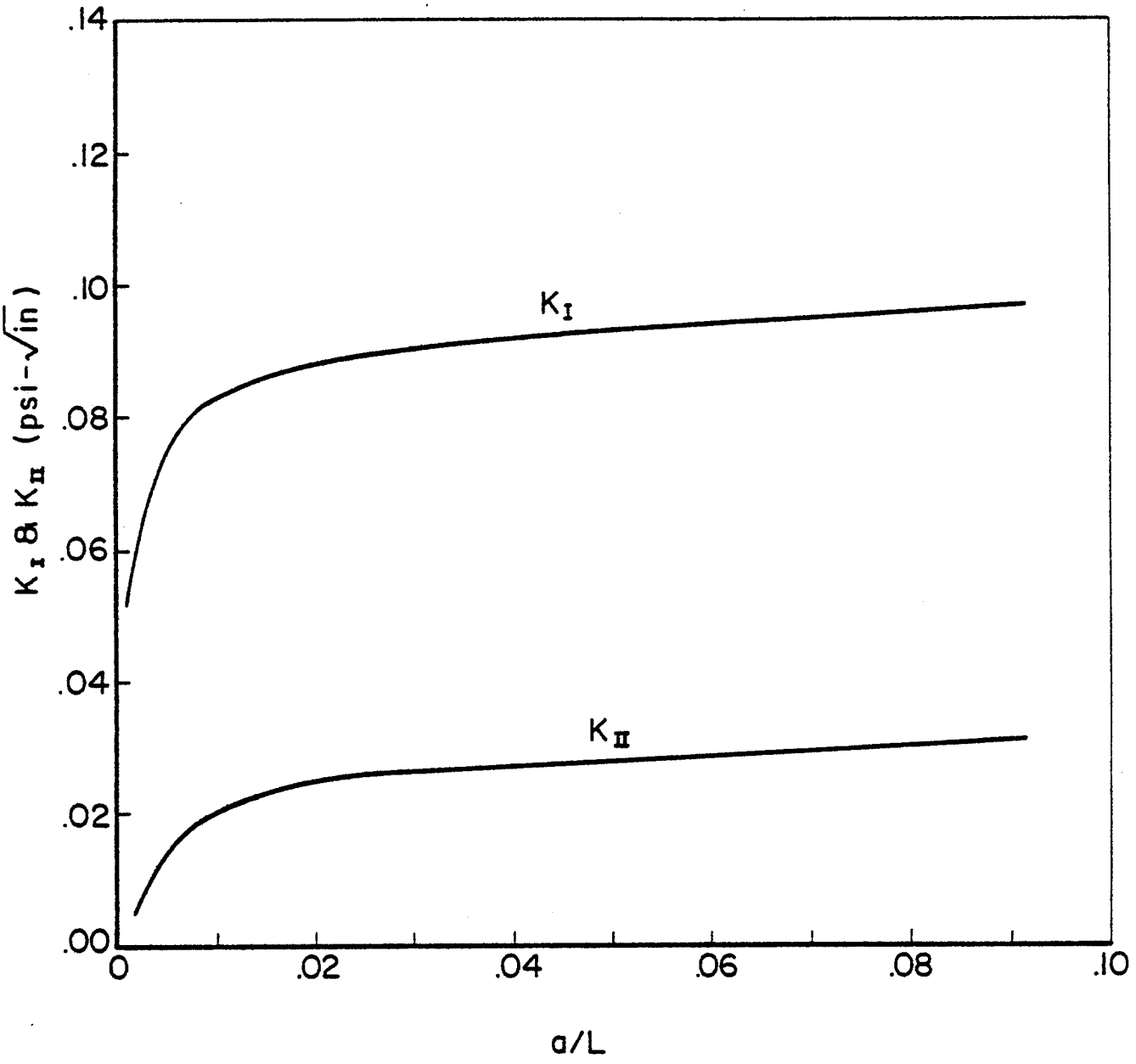

Fig. 11 Stress Intensity Factor Solutions Vs. Interface Crack Length in Lap Shear Adhesive Joints (L = 0.5 in., $E_1 = E_3 = 10\times10^6$ psi, $\nu_1 = \nu_3 = 0.33$, $E_2 = 0.5\times10^6$ psi, $\nu_2 = 0.35$)

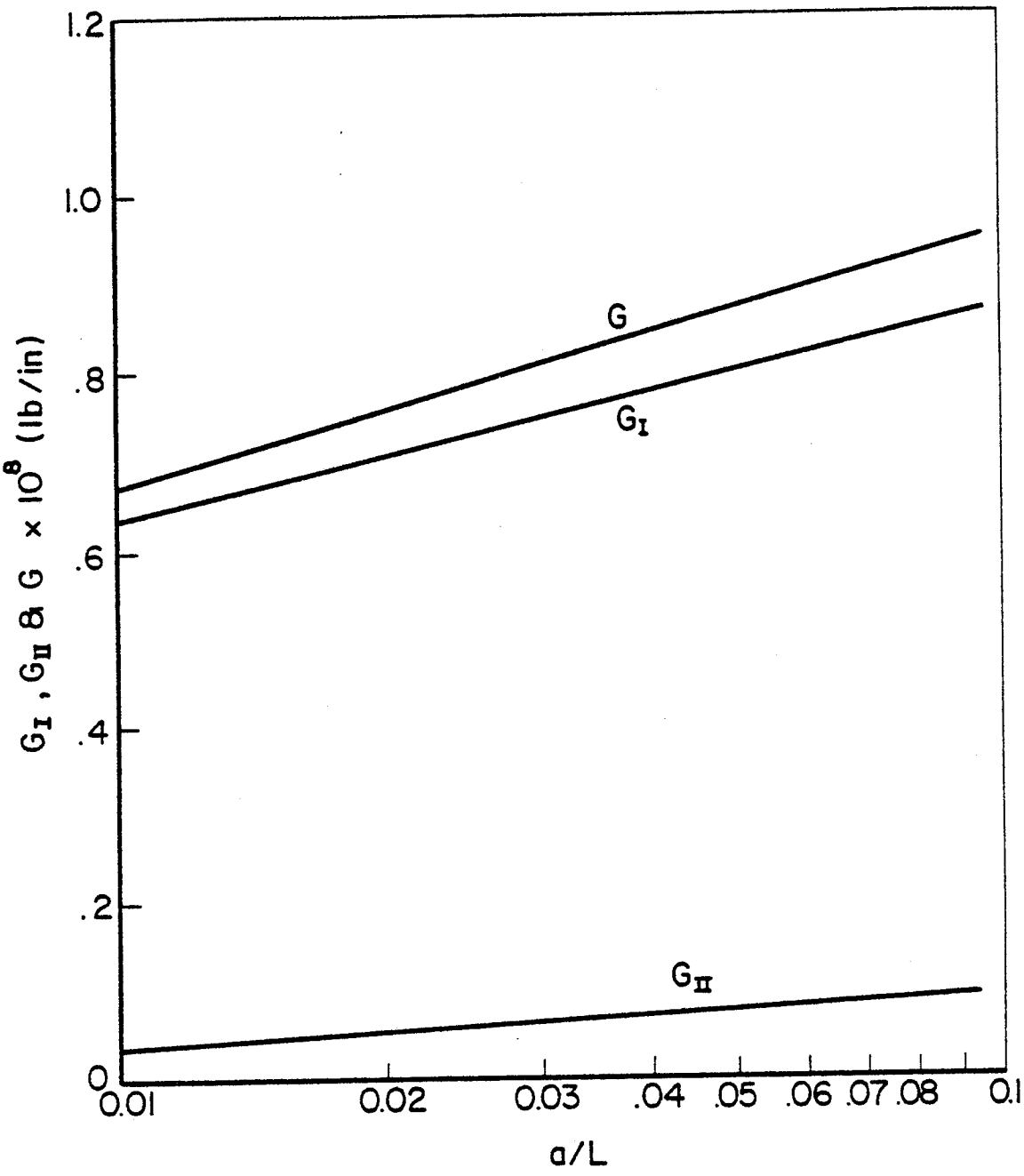

Fig. 12 Energy Release Rates Vs. Interface Crack Length in Lap Shear Adhesive Joints (L = 0.5 in., $E_1 = E_3 = 10\times10^6$ psi, $\nu_1 = \nu_3 = 0.33$, $E_2 = 0.5\times10^6$ psi, $\nu_2 = 0.35$)

FINAL REPORT - PART IV - DISTRIBUTION LIST

NSG 3044

ANALYSIS OF INTERFACE CRACKS IN ADHESIVELY BONDED LAP SHEAR JOINTS

NASA CR 165438

Advanced Research Projects Agency
Washington DC 20525
Attn: Library

Advanced Technology Center, Inc.
LTV Aerospace Corporation
P.O. Box 6144
Dallas, TX 75222
Attn: D. H. Petersen
W. J. Renton

Air Force Flight Dynamics Laboratory
Wright-Patterson Air Force Base, OH 45433
Attn: E. E. Baily
G. P. Sendeckyj (FBC)
R. S. Sandhu

Air Force Materials Laboratory
Wright-Patterson Air Force Base, OH 45433
Attn: H. S. Schwartz (LN)
T. J. Reinhart (MBC)
G. P. Peterson (LC)
E. J. Morrisey (LAE)
S. W. Tsai (MBM)
N. J. Pagano
J. M. Whitney (MBM)

Air Force Office of Scientific Research
Washington DC 20333
Attn: J. F. Masi (SREP)

Air Force Office of Scientific Research
1400 Wilson Blvd.
Arlington, VA 22209

AFOSR/NA
Bolling AFB, DC 20332
Attn: A. K. Amos

Air Force Rocket Propulsion Laboratory
Edwards, CA 93523
Attn: Library

Babcock & Wilcox Company
Advanced Composites Department
P.O. Box 419
Alliance, Ohio 44601
Attn: P. M. Leopold

Bell Helicopter Company
P.O. Box 482
Ft. Worth, TX 76101
Attn: H. Zinberg

The Boeing Company
P. O. Box 3999
Seattle, WA 98124
Attn: J. T. Hoggatt, MS. 88-33
T. R. Porter

The Boeing Company
Vertol Division
Morton, PA 19070
Attn: E. C. Durchlaub

Battelle Memorial Institute
Columbus Laboratories
505 King Avenue
Columbus, OH 43201
Attn: L. E. Hulbert

Bendix Advanced Technology Center
9140 Old Annapolis Rd/Md. 108
Columbia, MD 21045
Attn: O. Hayden Griffin

Brunswick Corporation
Defense Products Division
P. O. Box 4594
43000 Industrial Avenue
Lincoln, NE 68504
Attn: R. Morse

Celanese Research Company
86 Morris Ave.
Summit, NJ 07901
Attn: H. S. Kliger

Commander
Natick Laboratories
U. S. Army
Natick, MA 01762
Attn: Library

Commander
Naval Air Systems Command
U. S. Navy Department
Washington DC 20360
Attn: M. Stander, AIR-43032D

Commander
Naval Ordnance Systems Command
U.S. Navy Department
Washington DC 20360
Attn: B. Drimmer, ORD-033
M. Kinna, ORD-033A

Cornell University
Dept. Theoretical & Applied Mech.
Thurston Hall
Ithaca, NY 14853
Attn: S. L. Phoenix

Defense Metals Information Center
Battelle Memorial Institute
Columbus Laboratories
505 King Avenue
Columbus, OH 43201

Department of the Army
U.S. Army Aviation Materials Laboratory
Ft. Eustis, VA 23604
Attn: I. E. Figge, Sr.
Library

Department of the Army
U.S. Army Aviation Systems Command
P.O. Box 209
St. Louis, MO 63166
Attn: R. Vollmer, AMSAV-A-UE

Department of the Army
Plastics Technical Evaluation Center
Picatinny Arsenal
Dover, NJ 07801
Attn: H. E. Pebly, Jr.

Department of the Army
Watervliet Arsenal
Watervliet, NY 12189
Attn: G. D'Andrea

Department of the Army
Watertown Arsenal
Watertown, MA 02172
Attn: A. Thomas

Department of the Army
Redstone Arsenal
Huntsville, AL 35809
Attn: R. J. Thompson, AMSMI-RSS

Department of the Navy
Naval Ordnance Laboratory
White Oak
Silver Spring, MD 20910
Attn: R. Simon

Department of the Navy
U.S. Naval Ship R&D Laboratory
Annapolis, MD 21402
Attn: C. Hersner, Code 2724

Director
Deep Submergence Systems Project
6900 Wisconsin Avenue
Washington DC 20015
Attn: H. Bernstein, DSSP-221

Director
Naval Research Laboratory
Washington DC 20390
Attn: Code 8430
I. Wolock, Code 8433

Drexel University
32nd and Chestnut Streets
Philadelphia, PA 19104
Attn: P. C. Chou

E. I. DuPont DeNemours & Co.
DuPont Experimental Station
Wilmington, DE 19898
Attn: D. L. G. Sturgeon

Fiber Science, Inc.
245 East 157 Street
Gardena, CA 90248
Attn: E. Dunahoo

General Dynamics
P.O. Box 748
Ft. Worth, TX 76100
Attn: D. J. Wilkins
Library

General Dynamics/Convair
P.O. Box 1128
San Diego, CA 92112
Attn: J. L. Christian
R. Adsit

General Electric Co.
Evendale, OH 45215
Attn: C. Stotler
R. Ravenhall

General Motors Corporation
Detroit Diesel-Allison Division
Indianapolis, IN 46244
Attn: M. Herman

Georgia Institute of Technology
School of Aerospace Engineering
Atlanta, GA 30332
Attn: L. W. Rehfield

Grumman Aerospace Corporation
Bethpage, Long Island, NY 11714
Attn: S. Dastin
J. B. Whiteside

Hamilton Standard Division
United Aircraft Corporation
Windsor Locks, CT 06096
Attn: W. A. Percival

Hercules, Inc.
Allegheny Ballistics Laboratory
P. O. Box 210
Cumberland, MD 21053
Attn: A. A. Vicario

Hughes Aircraft Company
Culver City, CA 90230
Attn: A. Knoell

Illinois Institute of Technology
10 West 32 Street
Chicago, IL 60616
Attn: L. J. Broutman

IIT Research Institute
10 West 35 Street
Chicago, IL 60616
Attn: I. M. Daniel

Jet Propulsion Laboratory
4800 Oak Grove Drive
Pasadena, CA 91103
Attn: Library

Lawrence Livermore Laboratory
P.O. Box 808, L-421
Livermore, CA 94550
Attn: T. T. Chiao
E. M. Wu

Lehigh University
Institute of Fracture &
Solid Mechanics
Bethlehem, PA 18015
Attn: G. C. Sih

Lockheed-Georgia Co.
Advanced Composites Information Center
Dept. 72-14, Zone 402
Marietta, GA 30060
Attn: T. M. Hsu

Lockheed Missiles and Space Co.
P.O. Box 504
Sunnyvale, CA 94087
Attn: R. W. Fenn

Lockheed-California
Burbank, CA 91503
Attn: J. T. Ryder
K. N. Lauraitis
J. C. Ekvall

McDonnell Douglas Aircraft Corporation
P.O. Box 516
Lambert Field, MS 63166
Attn: J. C. Watson

McDonnell Douglas Aircraft Corporation
3855 Lakewood Blvd.
Long Beach, CA 90810
Attn: L. B. Greszczuk

Material Sciences Corporation
1777 Walton Road
Blue Bell, PA 19422
Attn: B. W. Rosen

Massachusetts Institute of Technology
Cambridge, MA 02139
Attn: F. J. McGarry
J. F. Mandell
J. W. Mar

NASA-Ames Research Center
Moffett Field, CA 94035
Attn: Dr. J. Parker
Library

National Aeronautics & Space Administration
Office of Technology Utilization
Washington DC 20546

National Bureau of Standards
Eng. Mech. Section
Washington DC 20234
Attn: R. Mitchell

National Science Foundation
Engineering Division
1800 G. Street, NW
Washington DC 20540
Attn: Library

Northrop Corporation Aircraft Group
3901 West Broadway
Hawthorne, CA 90250
Attn: R. M. Verette
G. C. Grimes

Pratt & Whitney Aircraft
East Hartford, CT 06108
Attn: J. M. Woodward

Raytheon Co., Missile System Division
Mechanical Systems Laboratory
Bedford, MA
Attn: P. R. Digiovanni

Rensselaer Polytechnic Institute
Troy, NY 12181
Attn: R. Loewy

Rockwell International
Los Angeles Division
International Airport
Los Angles, CA 90009
Attn: L. M. Lackman
D. Y. Konishi

Sikorsky Aircraft Division
United Aircraft Corporation
Stratford, CT 06602
Attn: Library

Southern Methodist University
Dallas, TX 75275
Attn: R. M. Jones

Space & Missile Systems Organization
Air Force Unit Post Office
Los Angeles, CA 90045
Attn: Technical Data Center

NASA-Flight Research Center
P.O. Box 273
Edwards, CA 93523
Attn: Library

NASA-George C. Marshall Space Flight Center
Huntsville, AL 35812
Attn: C. E. Cataldo, S&E-ASTN-MX
Library

NASA-Goddard Space Flight Center
Greenbelt, MD 20771
Attn: Library

NASA-Langley Research Center
Hampton, VA 23365
Attn: J. H. Starnes
J. G. Davis, Jr.
M. C. Card
J. R. Davidson

NASA-Lewis Research Center
21000 Brookpark Road, Cleveland, OH 44135

Attn: Contracting Officer, MS 501-11
Tech. Report Control, MS 5-5
Tech. Utilization, MS 3-16
AFSC Liaison, MS 501-3
S&MTD Contract Files, MS 49-6
L. Berke, MS 49-6
N. T. Saunders, MS 49-1
R. F. Lark, MS 49-6
J. A. Ziemianski, MS 49-6
R. H. Johns, MS 49-6
C. C. Chamis, MS 49-6 (8 copies)
R. L. Thompson, MS 49-6
T. T. Serafini, MS 49-1
Library, MS 60-3 (2 copies)

NASA-Lyndon B. Johnson Space Center
Houston, TX 77001
Attn: S. Glorioso, SMD-ES52
Library

NASA Scientific and Tech. Information Facility
P.O. Box 8757
Balt/Wash International Airport, MD 21240
Attn: Acquisitions Branch (15 copies)

National Aeronautics & SpaceAdministration
Office of Advanced Research & Technology
Washington DC 20546
Attn: L. Harris, Code RTM-6
M. Greenfield, Code RTM-6
D. J. Weidman, Code RTM-6

Structural Composites Industries, Inc.
6344 N. Irwindale Avenue
Azusa, CA 91702
Attn: R. Gordon

Texas A&M
Mechanics & Materials Research Center
College Station, TX 77843
Attn: R. A. Schapery
Y. Weitsman

TRW, Inc.
23555 Euclid Avenue
Cleveland, OH 44117
Attn: I. J. Toth

Union Carbide Corporation
P. O. Box 6116
Cleveland, OH 44101
Attn: J. C. Bowman

United Technologies Research Center
East Hartford, CT 06108
Attn: R. C. Novak
Dr. A. Dennis

University of Dayton Research Institute
Dayton, OH 45409
Attn: R. W. Kim

University of Delaware
Mechanical & Aerospace Engineering
Newark, DE 19711
Attn: B. R. Pipes

University of Illinois
Department of Theoretical & Applied Mechanics
Urbana, IL 61801
Attn: S. S. Wang

University of Oklahoma
School of Aerospace Mechanical & Nuclear Engineering
Norman, OK 73069
Attn: C. W. Bert

University of Wyoming
College of Engineering
University Station Box 3295
Laramie, WY 82071
Attn: D. F. Adams

U. S. Army Materials & Mechanics Research Center
Watertown Arsenal
Watertown, MA 02172
Attn: E. M. Lenoe
D. W. Oplinger

V.P. I. and S. U.
Dept. of Eng. Mech.
Blacksburg, VA 24061
Attn: R. H. Heller
H. J. Brinson
C. T. Herakovich
K. L. Reifsnider